Unified description of the fission probability for higly excited nuclei

Hiroki IWAMOTO[†1]

[1]Nuclear Science and Engineering Center, Japan Atomic Energy Agency
[†]Email: iwamoto.hiroki@jaea.go.jp

This paper describes a summary of the spallation reaction and its theoretical model, focusing on the spallation product yields, and then our research work about the improvement of the fission probability model is presented.

1 Introduction

Recently, spallation neutrons produced from the spallation reactions have been utilized for the material and fundamental sciences as well as industrial applications in the spallation neutron source facilities (e.g. MLF at J-PARC [1, 2, 3], ISIS [4], and SNS [5]). In these facilities, Monte Carlo particle transport codes such as PHITS [6], MCNP [7], GEANT4 [8], FLUKA [9] play a significant role in the assessment of radiation dose and inventory of radioactive materials.

In this paper, we briefly describe the spallation reaction and its theoretical spallation model, focusing on spallation product yields; then, our research work on this title is presented.

2 Spallation reaction

2.1 Spallation reaction process

Figure 1 schematizes a process of the spallation reaction. The spallaion reaction starts with a collision between an incident particle and a nucleon which is a constituent of a nucleus. The bombarded nucleon emits solely from the nucleus, hit other nuclons several times, or emits binding to nucleons in the nuclear surface; this process is referred to as the intranuclear cascade process. After this process, the remaining energy is uniformly distributed by repeating soft collisions, which results in a quasi-stable, highly-excited state.

This highly-excited nucleus de-excites by statistically emitting neutrons, charged particles and photons; this process is referred to as the de-excitation process; this process is also known as the evaporation process. For heavy targets such as gold, lead, and uranium, fission occurrs competing with the evaporation.

2.2 Distribution of spallation products and spallation model

Figure 2 compares the mass number distribution of the spallation products produced from the 1-GeV proton-induced ^{208}Pb reaction between the experimental data [10] and calculation results with four major spallation models (i.e. INCL++/ABLA07 [11, 12], INCL++/GEMINI++ [13], INCL4.6/GEM [14], and CEM03.03 [15]). Three humps observed in this figure are referred to as evaporation residues (ER), fission fragments (FF), and light charged particles (LCP) in order of

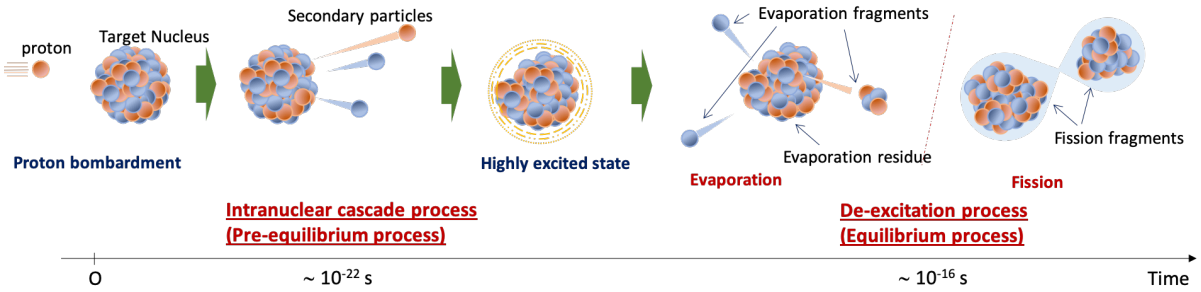

Figure 1: Process of the spallation reaction.

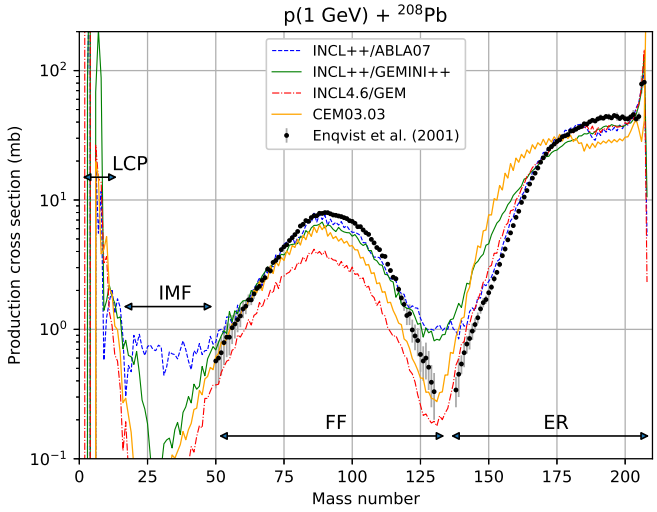

Figure 2: Mass number distribution of the 1-GeV proton-induced ^{208}Pb target reaction.

decreasing mass number. While all models explain the feature of the mass number distribution, they are not very good in terms of the prediction accuracy. For example, INCL4.6/GEM, which is a default spallation model of PHITS, underestimates the fission fragment yields by at most 50%. Because the fission fragments contains volatile radioactive materials such as radioactive kripton, xenon, and iodine, this underestimation may involve a significant problem in terms of the radiation safety of the spallation neutron source facilities. These discrepancies were discussed in detail in our previous work [16].

3 Improvement of fission probability

3.1 Description of fission probability

A recent benchmark analysis of the PHITS code revealed that INCL4.6/GEM implemented in PHITS underestimates the fission fragment yields. This underestimation indicates that the fission probability should be enhanced within the framework of the de-excitation model GEM.

The GEM describes the fission probability as follows.

$$P = \frac{\Gamma_f}{\Gamma_n + \Gamma_f}, \tag{1}$$

where Γ_f and Γ_n represent the decay widths of fission and neutron evaporation, respectively. Although parameters of these decay widths need to be sophisticated as a straightforward method, this approach requires a significant amount of time spent in tuning the model parameters. To avoid this, we modified the fission probability itself instead of the decay widths, which are deduced from a systematics of proton-induced fission cross sections.

The fission cross section $\sigma_{\rm fis}$ and non-elastic cross section $\sigma_{\rm nonel}$ are linked to the following equation:

$$\mathcal{P} = \frac{\sigma_{\rm fis}}{\sigma_{\rm nonel}}, \tag{2}$$

where $\mathcal{P}$ indicates a total fission probability, which can be calculated from the systematics of the proton-induced fission cross sections (Prokofiev systematics [17]) and that of the non-elastic cross sections (Pearlstein–Niita systematics [18]); both are functions of incident proton energy and mass and proton numbers of the target nucleus. However, what we are interested in here is the fission probability which is a function of excitation energy, mass number, and proton number of the highly excited nuleus. To resolve this discrepancy, relationships among information of projectile, target nuclei, and highly-excited nuclei are deduced statistically from the intranuclear cascade model calculation, and the fission probability was determined by multiplying the total fission probability with a function g:

$$P = g \cdot \mathcal{P}(\langle E_p \rangle, \langle Z_t \rangle, \langle A_t \rangle), \tag{3}$$

where $\langle E_p \rangle$, $\langle Z_t \rangle$, and $\langle A_t \rangle$ are the corresponding incident proton energy, proton number, and mass number, respectively. The function g is expressed as

$$g = \max\left(0, \gamma_0 \left(\frac{1}{1+\mathrm{e}^{-\gamma_1(E-\gamma_2)}} - \gamma_3\right)\right), \tag{4}$$

where $\gamma_i\,(i = 0, 1, 2, 3)$ is adjustable parameters to account for the proton-induced fission cross sections, which are expressed as

$$\gamma_0 = 0.46, \quad \gamma_1 = 0.10, \quad \gamma_2 = 57\left(\frac{X_{^{208}\mathrm{Pb}}}{\langle X_t \rangle}\right)^{5.5}, \quad \gamma_3 = \frac{1}{2}\left(\frac{X_{^{208}\mathrm{Pb}}}{\langle X_t \rangle}\right)^{3}, \tag{5}$$

where $X_{^{208}\mathrm{Pb}}$ and $\langle X_t \rangle$ are the fissility parameter for ^{208}Pb and the corresponding fissility parameter for the highly-excited nucleus.

3.2 Results

3.2.1 Fission cross sections

Figure 3 shows examples of the proton-induced and neutron-induced fission cross sections calculated by the proposed model. It is seen that the proposed model reproduces the experimental data fairly well, in contrast to the conventional model. Furthermore, even though this model is constructed by the proton-induced systematics, it is applicable the neutron-induced reactions. It was demonstrated that our model reproduces the experimental fission cross sections over a wide range of subactinide targets for proton-, neutron-, and deuteron-induced reactions. Details can be seen in Iwamoto et al. [19].

3.2.2 Fission fragment production cross sections

Figure 4 presents the proton-induced fission fragment production cross sections for the 1-GeV ^{208}Pb(p, X), 800-MeV ^{197}Au(p, X), and 500-MeV ^{208}Pb(p, X) reactions. Note that both the

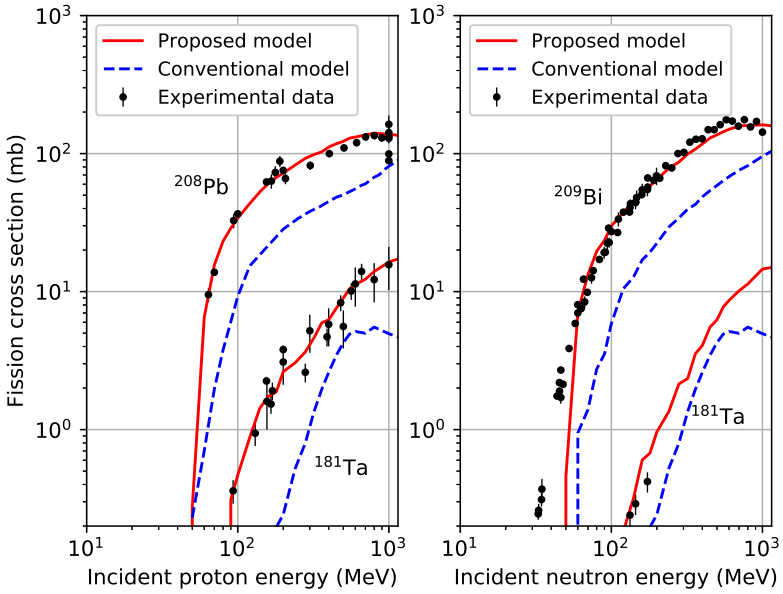

Figure 3: Proton-induced and neutron-induced fission cross sections.

calculated and experimental cross sections indicates independent yields. Although our proposed model can provide the fission cross sections, namely the total fission fragment production cross sections, with markededly improved accuracy, it is observed from this figure that each peak for element uniformly shifts to heavy mass numbers. This means that the fission fragments were computationally produced as uniformly neutron-rich states. The left panels of Figure 5 shows $\langle N \rangle / Z$ distributions for the three reactions, comparing between the conventional and proposed models, in which the modified model becomes worse with respect to the $\langle N \rangle / Z$ distributions. As shown in the right panel of Figure 5, we found that this discrepancy is reduced by emitting three neutrons ($\nu = 3$) from the fissioning system. Because the neutron emission is considered to be driven by the excitation energy, we investigated how much excitation energy is required to account for the $\langle N \rangle / Z$ distributions. As a result, it was suggested that excitation energy of about 30–50 MeV is required, which would be consistent with a value deduced from the neutron separation energy; if the separation energy is assumed to be 8 MeV, the minimum energy of the three neutron emission becomes 24 MeV.

4 Conclusions

We have described the spallation reaction and its theoretical spallation model, focusing on spallation product yields, and our research work have been presented. Recently, experimental studies on the spallation reaction have become active in Japan [20, 21, 22]. We hope that the combination of our theretical work and these experiemntal activities will lead to a deeper understanding of the spallation reaction mechanism.

References

[1] Takada, H, et al., Quant. Beam Sci. **1**(2), 2017, pp.8-1–8-26.

[2] Nakajima, K, et al., Quant. Beam Sci. **1**(3), 2017, pp.9-1–10-59.

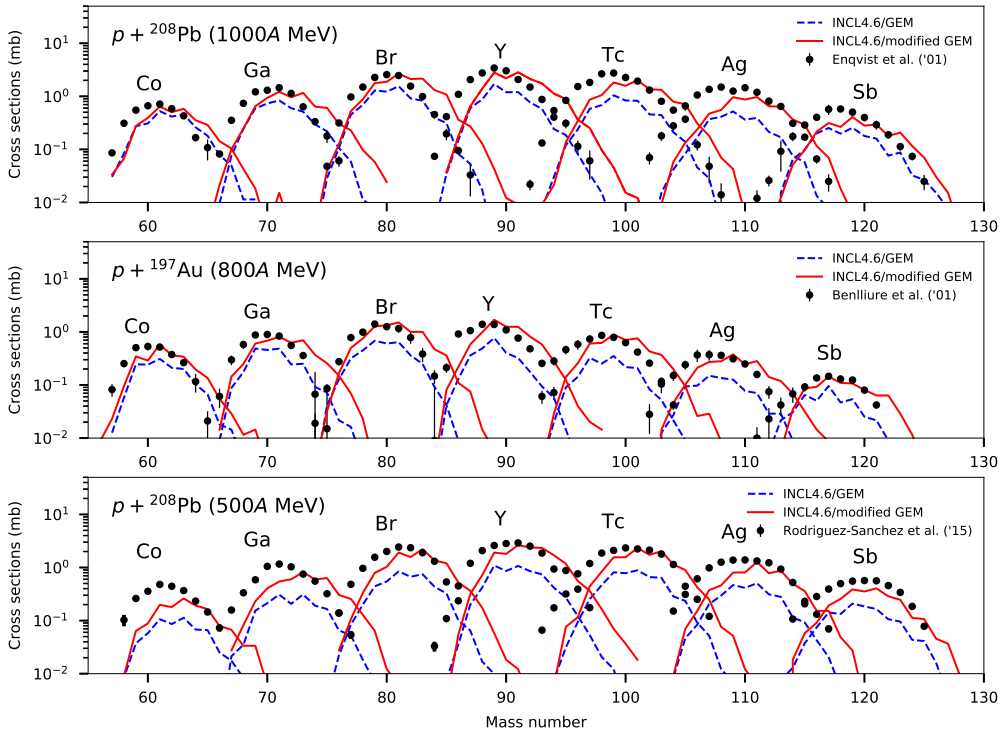

Figure 4: Proton-induced fission fragment production cross sections. Experimental data were taken from Enqvist et al. [10]

[3] Sakasai, K, et al., Quant. Beam Sci. **1**(2), 2017, pp.10-1–10-35.

[4] Thomason, J.W.G., Nucl. Instr. Meth. Phys. Res. A **917**, 2019, pp.61–67.

[5] Mason, T.E., et. al., Phys. B Condens. Matter **385–386**(2), 2006, pp.955–960.

[6] Sato, T., et al., J. Nucl. Sci. Technol. **55**;12, 2018, pp.529–533.

[7] Werner, C.J., et al. Los Alamos National Laboratory report LA-UR-17-29981, 2018.

[8] Allison, J., et al., Nucl. Instr. Meth. Phys. Res. A **835**, 2016, pp.186–225.

[9] Böhlen, T.T., et al., Nucl. Data Sheets **120**, 2014, pp.211–214.

[10] Enqvist, T., et al. Nucl. Phys. A. **686**, 2001, pp.481-–524.

[11] Leray, S., et al., J. Phys.: Conf. Series **420**, 2013, pp.012065.

[12] Kelič, A., et al., INDC(NDS)-0530, IAEA, 2008.

[13] Charity, R.J., Phys. Rev. C **82**, 2010, pp.014610.

[14] Furihata, S., et al., JAERI-Data/Code 2001-015, 2001.

[15] Mashnik, S.G., Nucl. Phys. A **568**, 1994, pp.703–726.

[16] Iwamoto, H., et al., EPJ Web of Conf. **239**, 2020, pp.06001.

[17] Prokofiev, A.V., Nucl. Instr. Meth. Phys. Res. A **463**, 2001, pp.557–575.

[18] Niita, K., et al., Nucl. Instr. Meth. Phys. Res. B **184**, 2001, pp.406–420.

[19] Iwamoto, H., Meigo, S., J. Nucl. Sci. Technol. **56**;2, 2018, pp.160–171.

[20] Matsuda, H., et al., J. Nucl. Sci. Technol. **55**;8, 2018, pp.955–961.

[21] Matsuda, H., et al., Nucl. Instr. Meth. Phys. Res. A **483**, 2020, pp.33–40.

[22] Wang, H., et al., Phys. Lett. B **754**, 2016, pp.104–108.

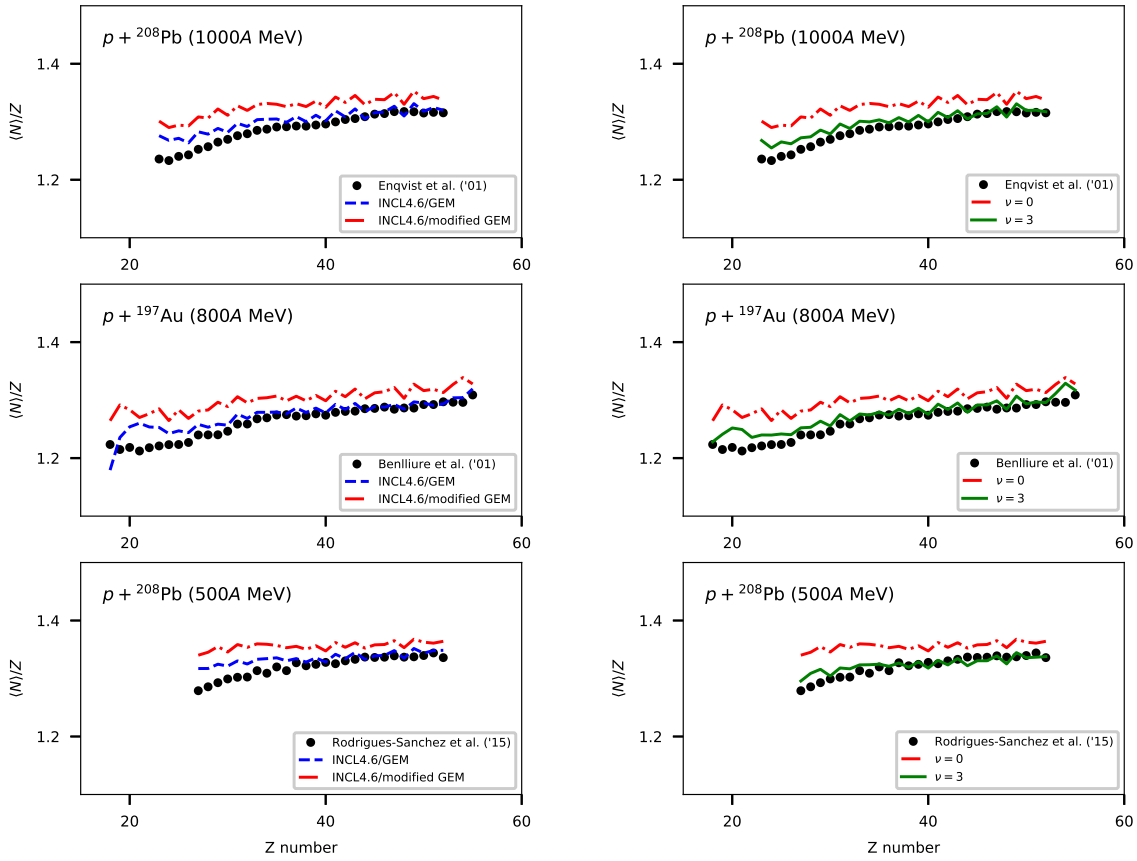

Figure 5: $\langle N \rangle / Z$ distributions as a function of Z number. The left panels show comparison between the conventional and proposed models; the right panels show comparison of the calculation results between $\nu = 0$ and $\nu = 3$, where ν is the number of neutron emission.

Acknowledgements

The author would like to acknowledge many helpful discussions with the co-author of this work [19], Dr. S. Meigo, and Drs. K. Nihsio, T. Sato, T. Ogawa, S. Hashimoto, Y. Iwamoto, T. Fukahori, and T. Kawano. This work was supported by Japan Society fort the Promotion of Science (JSPS) Grants-in-Aid for Young Scientists B [grant number 17K14916].